applied sciences

MDPI

Article

Evolution of Floor Rockburst Instability Tendency and Optimization of Borehole Pressure-Relief Horizons in Roadways with Retained Bottom Coal

Wenyu Lyu [1], Xinxin Zhou [1], Zhenhua Ouyang [2,3,*], Ranran Zhou [4], Yongping Wu [1], Panshi Xie [1], Ru You [1], Shiji Ma [2], Gen Li [1], Haiyang Yi [2] and Ningbo Zhang [2]

[1] College of Energy and Mining Engineering, Xi'an University of Science and Technology, Xi'an 710054, China; lvwenyu@xust.edu.cn (W.L.); zxx08522580@163.com (X.Z.); wuy-9/p@xust.edu.cn (Y.W.); xieps@xust.edu.cn (P.X.); you.ru@stu.xust.edu.cn (R.Y.); lg970426@163.com (G.L.)
[2] College of Mine Safety, University of Emergency Management, Langfang 065201, China; 19862131402@163.com (S.M.); yihaiyangchina@gmail.com (H.Y.); znb444@sina.com (N.Z.)
[3] Key Laboratory of Drilling Technology in Mine Rescue, Ministry of Emergency Management, Beijing 100040, China
[4] Zhundong-Xinjiang Economic and Technological Development Zone Management Committee, Changji 831700, China; zrrzrr916@163.com
* Correspondence: oyzhua@163.com; Tel.: +86-18611732595

Abstract

To investigate the evolution of floor rockburst instability tendency and optimize borehole pressure-relief horizons in roadways with retained bottom coal, theoretical analysis and numerical simulation were employed to investigate the effects of bottom coal thickness on composite-floor stability, load-bearing and energy-storage states, and borehole pressure-relief response. Based on the equivalent transformed-section method, a stability analysis model for the bottom coal–floor composite structure was established to reveal the mechanism by which increasing bottom coal thickness reduces structural stability and influences the floor instability tendency. Numerical results show that, with increasing bottom coal thickness, the dominant load-bearing and energy-storage response progressively shifts from the floor strata to the bottom coal–floor composite structure and then to thick bottom coal. An energy–stress index K was introduced to characterize the transition in the load-bearing and energy-storage states of the composite floor. Further analysis of the effect of borehole vertical depth indicates that pressure-relief effectiveness depends on the spatial matching between the weakened zone and the main load-bearing and energy-storage zones, rather than on indiscriminately increasing borehole depth. Under the simulated conditions, the reasonable borehole vertical depth ranges from 3.0 to 4.0 m for a bottom coal thickness of 2 m and from 4.0 to 5.0 m for bottom coal thicknesses of 4, 6, and 8 m. The results provide a theoretical reference for understanding the relative evolution of floor rockburst instability tendency and optimizing borehole pressure-relief horizons in roadways with retained bottom coal.

Keywords: roadways with retained bottom coal; composite-floor stability; load-bearing and energy-storage states; energy-stress index; borehole pressure-relief horizons

Check for updates

Academic Editor: Nikolaos Koukouzas

Received: 17 September 2026
Revised: 23 October 2026
Accepted: 23 October 2026
Published: 28 October 2026

Copyright: © 2026 by the authors. Licensee MDPI, Basel, Switzerland. This article is an open access article distributed under the terms and conditions of the Creative Commons Attribution (CC BY) license.

1. Introduction

With the continuous increase in coal mining depth, stress levels in roadway surrounding rock continue to rise, and dynamic disasters such as rockbursts have become increasingly

prominent [1–4]. The floor is a relatively weak component of the roadway surrounding-rock support system and is prone to dynamic failure, including instantaneous floor heave, cracking, and coal-rock ejection, under high horizontal stress and mining-induced disturbance [5–7]. Owing to coal seam occurrence conditions, geological structures, and mining methods, a certain thickness of bottom coal is often retained beneath the roadway, which can aggravate floor rockburst risk [8–10]. Therefore, studying the floor rockburst instability mechanism and control technologies for roadways with retained bottom coal is of great significance for mine safety.

Regarding floor rockburst instability mechanisms, Xiao et al. [11] established a mechanical model of floor rockburst instability, derived an energy criterion for roadway floor rockburst instability, and identified horizontal stress as a major inducing factor. Mu et al. [12] developed a dynamic floor-fracture model based on elastic thin-plate theory and showed that roadway width and horizontal stress are important factors influencing floor failure. Zhang et al. [13] suggested that high static loading provides the internal basis for floor heave deformation, whereas strong dynamic disturbance acts as an important trigger for floor rockburst instability. Zhou et al. [14] and Liu et al. [15] revealed floor failure mechanisms under superimposed static and dynamic loading from the perspectives of stress transfer and buckling instability, respectively. Feng et al. [16], Xu et al. [17], and Wang et al. [18] further indicate that mining-induced stress, dynamic disturbance, and reduced structural stability are important factors governing floor rockburst instability.

Regarding bottom coal thickness and the stability of coal-rock composite floors, Tan et al. [19] showed that bottom coal thickness and mechanical properties significantly affect floor stress, elastic strain energy, and deformation. Zhang et al. [20] analyzed the influence of bottom coal thinner than 3 m on floor rockburst and found that, under thin-bottom-coal conditions, the floor strata act as the main energy-storage body, whereas the bottom coal is an important medium for dynamic manifestation. Chen et al. [21] reported that increasing bottom coal thickness increases the risk of floor instability under dynamic disturbance. Chang et al. [22] and Mo et al. [23] analyzed composite-floor deformation and instability from the perspectives of stress transfer across the coal-rock interface and the structural combination of hard and weak strata, respectively. These studies demonstrate that bottom coal thickness alters the bottom coal–floor composite structure and its load-bearing and energy-storage characteristics; however, the evolution of the dominant load-bearing and energy-storage media and the associated rockburst instability tendency under different bottom coal thicknesses requires further investigation.

Regarding floor pressure relief and rockburst prevention, blasting pressure relief, water-jet slotting, large-diameter boreholes, and grooving have been used to reduce floor stress concentration and elastic strain energy accumulation [24–28]. Chen et al. [29] further analyzed the energy-release and risk-reduction mechanism of floor boreholes, investigated the effects of borehole diameter, inclination, spacing, and row spacing on pressure-relief performance, and proposed reasonable values for the pressure-relief parameters. However, existing studies have focused mainly on pressure-relief methods and technical parameter optimization, whereas the reasonable borehole pressure-relief horizon of the roadway floor under different bottom coal thicknesses has received comparatively limited attention.

In summary, existing studies have mainly investigated the influence of bottom coal thickness on floor stability from the perspectives of stress, energy, and deformation indices. However, the understanding of structural stiffness variation in composite floors and the evolution characteristics of their load-bearing and energy-storage states under different bottom coal thicknesses remains insufficient. Moreover, the basis for determining reasonable borehole pressure-relief horizons has rarely been discussed from the perspective of weakening the critical load-bearing and energy-storage control regions of composite floors.

Accordingly, this study adopts the composite-section equivalence method to reveal the intrinsic mechanism by which bottom coal thickness influences composite-floor stability. Combined with numerical simulation, the migration characteristics of key load-bearing and energy-storage control regions under different bottom coal thicknesses are clarified. Furthermore, the influence of borehole vertical depth on the load-bearing and energy-storage state of the floor is analyzed, and an optimization method for borehole pressure-relief horizons based on the identification of key control regions is proposed. The findings provide a theoretical reference for understanding the relative evolution of floor rockburst instability tendency and optimizing borehole pressure-relief horizons in roadways with retained bottom coal.

2. Evolution Mechanism of Composite Floor Stability in Roadways with Retained Bottom Coal

2.1. Composite Floor Stability Analysis Model

After roadway excavation, the stress state of the surrounding rock is redistributed. The coal masses in the two ribs mainly carry the overburden load, while the roof and floor coal-rock masses are subjected to relatively high horizontal compressive stress under the constraint of the two ribs. Therefore, horizontal compressive stress is an important factor inducing floor extrusion deformation and structural instability. In engineering practice, the roadway floor is generally not composed of a single rock layer, but rather a layered coal-rock composite structure consisting of upper retained bottom coal and underlying floor strata. To analyze the stability of the retained bottom coal–floor composite structure under horizontal loading, a mechanical analysis model of the composite floor was established, as shown in Figure 1.

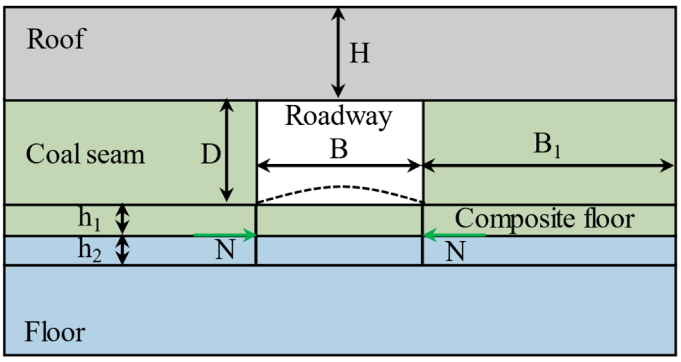


Figure 1. Mechanical analysis model of the composite floor in roadways with retained bottom coal. The dashed line represents the deflected profile of the composite floor, and the green arrows indicate the horizontal compressive forces acting on the composite floor.

The load within the load-bearing range of the rib coal is mainly composed of the self-weight of the overlying strata and the additional load transferred from the exposed roof of the adjacent goaf. Considering the approximate symmetry of the roadway, the vertical stress σ_y of the rib coal can be expressed as [30]:

$$\sigma_y = \alpha \frac{\left(B_1 + \frac{B}{2}\right) H\gamma_r + B_1 D\gamma_m}{B_1} \quad (1)$$

Vertical stress induces horizontal stress in the roadway floor via the Poisson effect and tectonic stress. The horizontal stress σ_x in the roadway floor can be expressed as:

$$\sigma_x = \alpha\beta\lambda \frac{\left(B_1 + \frac{B}{2}\right) H\gamma_r + B_1 D\gamma_m}{B_1} \quad (2)$$

Since the term $D\gamma_m$ in Equation (2) is relatively small, its effect can be neglected. Taking a unit length along the roadway axis, the horizontal axial pressure N acting at both ends of the composite floor can be expressed as:

$$N = \alpha\beta\lambda \frac{\left(B_1 + \frac{B}{2}\right)H\gamma_r}{B_1}(h_1 + h_2) \tag{3}$$

where B_1 is the load-bearing range of the rib coal, m; B is the roadway width, m; D is the roadway height, m; H is the distance from the roadway roof to the ground surface, m; γ_r is the average unit weight of the overlying strata, N·m^{-3}; γ_m is the unit weight of the coal seam, N·m^{-3}; α is the influence coefficient of the abutment pressure of the goaf roof; β is the influence coefficient of horizontal tectonic stress; λ is the lateral pressure coefficient, $\lambda = \frac{\mu}{1-\mu}$; μ is Poisson's ratio; h_1 is the bottom coal thickness, m; and h_2 is the thickness of the underlying floor strata, m.

Equation (3) gives the actual horizontal axial load acting on the composite floor after roadway excavation. The resistance of the composite floor to horizontal extrusion deformation depends not only on the magnitude of the horizontal axial pressure but also on the flexural stiffness of the structure itself. Considering that the actual roadway floor is a continuous coal-rock composite structure constrained by the surrounding rock, rather than an ideal slender column, the classical Euler theory is not adopted to calculate the absolute critical load [31,32]. Instead, this study focuses on the variation characteristics of the structural stiffness of composite floors under different bottom coal thicknesses.

For roadways with retained bottom coal, the mechanical properties of the bottom coal and underlying floor strata are different, and variations in bottom coal thickness alter the position of the neutral axis and the flexural stiffness of the composite section. Therefore, the equivalent transformed-section method is adopted to characterize the equivalent flexural stiffness of the bottom coal–floor composite structure, thereby analyzing the influence of bottom coal thickness on the deformation resistance of the composite structure.

It is assumed that the bottom coal and floor strata are both linearly elastic and isotropic, that the interface is well bonded, that deformation compatibility is maintained during bending, and that interlayer slip is neglected. According to mechanics of materials [32], let the bottom coal thickness be h_1, with elastic modulus E_1, and let the thickness of the underlying floor strata be h_2, with elastic modulus E_2. Taking the floor strata as the reference material, the elastic modulus ratio between the bottom coal and floor strata is $n = \frac{E_1}{E_2}$. Taking the floor strata width as $b = 1$ (unit length), the equivalent width of the bottom coal is $b_1 = nb = n$.

The total area A_c of the equivalent composite-floor section is:

$$A_c = nh_1 + h_2 \tag{4}$$

The distance y_c from the centroid of the composite section to the bottom surface is:

$$y_c = \frac{nh_1\left(h_2 + \frac{h_1}{2}\right) + h_2 \cdot \frac{h_2}{2}}{nh_1 + h_2} \tag{5}$$

According to the parallel-axis theorem, the second moment of area I_c of the composite section about the neutral axis is:

$$I_c = \left[\frac{1}{12}h_2^3 + h_2\left(y_c - \frac{h_2}{2}\right)^2\right] + n\left[\frac{1}{12}h_1^3 + h_1\left(h_2 + \frac{h_1}{2} - y_c\right)^2\right] \tag{6}$$

Based on the equivalent second moment of area of the composite section, the equivalent flexural stiffness D_c of the composite floor can be further obtained.

$$D_c = E_2 I_c \tag{7}$$

Thus, Equation (3) determines the actual horizontal axial pressure acting on the composite floor, whereas Equation (7) determines the equivalent flexural stiffness of the composite structure. Under the same roadway burial depth, cross-sectional dimensions, and in situ stress conditions, the influence range of excavation disturbance is considered relatively limited. Therefore, the total thickness of the bottom coal–floor composite structure can be regarded as constant, and variations in bottom coal thickness mainly alter the material composition and structural stiffness of the composite floor rather than significantly changing the external horizontal loading condition. Accordingly, the evolution characteristics of the flexural stiffness of the composite floor under different bottom coal thicknesses are further analyzed.

2.2. Effect of Bottom Coal Thickness on the Equivalent Flexural Stiffness of the Composite Floor

Assuming a rectangular roadway with a height of 4.0 m and a width of 5.0 m, the equivalent circular radius of the roadway section is approximately 2.52 m. The excavation disturbance range is taken as five times the equivalent circular radius, i.e., approximately 12.6 m. After subtracting the equivalent circular radius of the roadway, the thickness of the bottom coal–floor composite structure affected by excavation disturbance is determined to be approximately 10 m. Since bottom coal generally has a lower elastic modulus than the underlying floor strata, the elastic modulus of the floor strata is set as 2.3 GPa. The modulus ratios are assumed as 0.1, 0.2, 0.3, 0.4, and 0.5, and the evolution characteristics of the equivalent flexural stiffness of the composite floor under different bottom coal thicknesses are calculated, as shown in Figure 2.

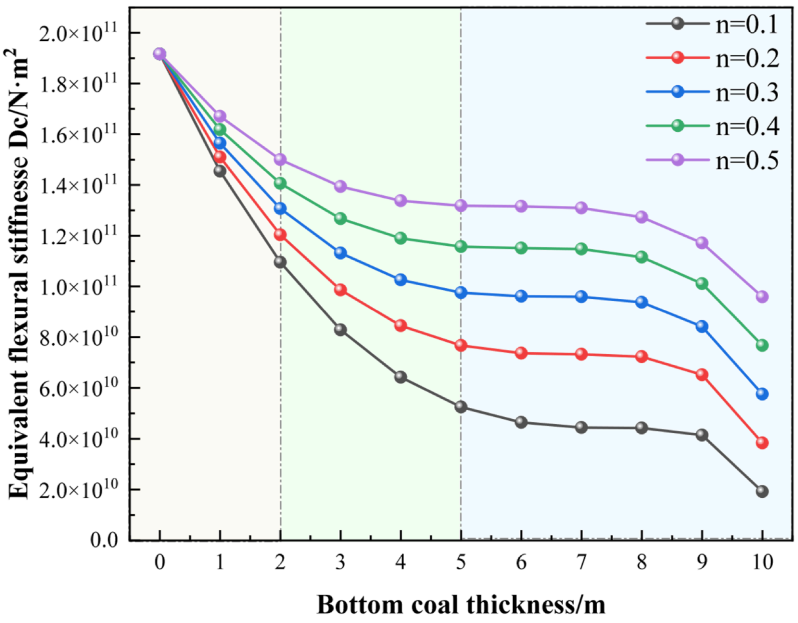


Figure 2. Evolution of the equivalent flexural stiffness of the composite floor under different bottom coal thicknesses.

As shown in Figure 2, the equivalent flexural stiffness of the composite floor continuously decreases with increasing bottom coal thickness, indicating that an increase in the proportion of bottom coal significantly weakens the deformation resistance of the bottom coal–floor composite structure. The difference in elastic modulus between bottom coal and floor strata mainly affects the degree of stiffness degradation.

When the bottom coal thickness ranges from 0 to 2 m, the bottom coal begins to participate in the bearing and deformation process of the composite floor. The equivalent flexural stiffness decreases rapidly; however, due to the relatively small thickness of bottom

coal, the high-stiffness floor strata still account for a large proportion of the composite structure. Therefore, the composite floor maintains relatively high deformation resistance, and the reduction in structural stability is relatively limited.

When the bottom coal thickness increases to 2–5 m, the proportion of bottom coal within the composite floor further increases, and the control of the equivalent flexural stiffness gradually shifts from the floor strata-dominated structure to the joint control of the coal-rock composite structure. Meanwhile, the contribution of the floor strata to the overall flexural stiffness gradually weakens. Although the degradation rate of equivalent flexural stiffness varies within this stage, the composite structure has entered a relatively low-stiffness state, resulting in further reduction in deformation resistance and increased sensitivity to external stress disturbance.

When the bottom coal thickness increases to 5–10 m, bottom coal gradually becomes the dominant component of the composite floor. The controlling role of the composite structure transitions from the coal-rock combination to thick bottom coal, and the variation trend of the equivalent flexural stiffness gradually becomes stable while maintaining a relatively low level. This indicates that the deformation resistance of the composite structure is significantly weakened under thick bottom coal conditions.

In summary, bottom coal thickness regulates the overall stiffness of the composite floor by changing the material composition and stiffness distribution of the bottom coal–floor composite structure. With increasing bottom coal thickness, the position of the neutral axis and the second moment of area of the composite section are altered, resulting in a reduction in the equivalent flexural stiffness of the composite floor and weakened resistance to horizontal extrusion deformation. Under the same horizontal loading condition, the composite floor is more prone to larger deformation, leading to reduced structural stability. This provides an important mechanical explanation for the increase in floor rockburst instability tendency with increasing bottom coal thickness. Therefore, under deep high-stress conditions and mining-induced disturbances, roadways with retained bottom coal are more likely to experience large deformation and instability failure, resulting in an increased tendency toward floor rockburst instability.

It should be noted that the theoretical model simplifies the actual floor structure of roadways with retained bottom coal. In this model, the bottom coal and floor strata are assumed to be linearly elastic and isotropic materials, and continuous contact between them is assumed. Complex factors such as interlayer slip, interface weakening, plastic failure of coal-rock masses, and external dynamic disturbances are not considered. Therefore, the theoretical analysis mainly focuses on the influence of bottom coal thickness on the evolution characteristics of the equivalent flexural stiffness and structural stability of the composite floor. The theoretical results are intended to reveal the underlying mechanism that increasing bottom coal thickness increases the proportion of low-stiffness coal, leading to stiffness degradation and reduced deformation resistance of the composite structure, rather than predicting the absolute critical condition of floor instability. Numerical simulation is further conducted to analyze the stress and energy evolution characteristics of the floor under different bottom coal thicknesses, thereby complementing the theoretical analysis.

3. Evolution of Load-Bearing and Energy-Storage Characteristics and Rockburst Instability Tendency of Floors in Roadways with Retained Bottom Coal

3.1. Numerical Model and Simulation Scheme

To further investigate how bottom coal thickness affects floor load-bearing and energy-storage characteristics and rockburst instability tendency, a numerical model was established using FLAC3D 7.0, as shown in Figure 3. The model dimensions are 50 m in length, 20 m

in width, and 45 m in height, and the roadway cross-section is 5.0 m wide and 4.0 m high. To facilitate comparison among cases, the roadway position was kept fixed, while bottom coal thickness was varied by adjusting the ranges assigned to the coal seam and floor strata properties. To cover the structural transition from no bottom coal and thin bottom coal to a coal-rock composite floor and a thick-bottom-coal-dominated floor, bottom coal thicknesses from 0 to 10 m were considered at 1.0 m intervals. A vertical monitoring line was arranged beneath the roadway center to extract stress and energy evolution characteristics of the floor coal-rock mass.

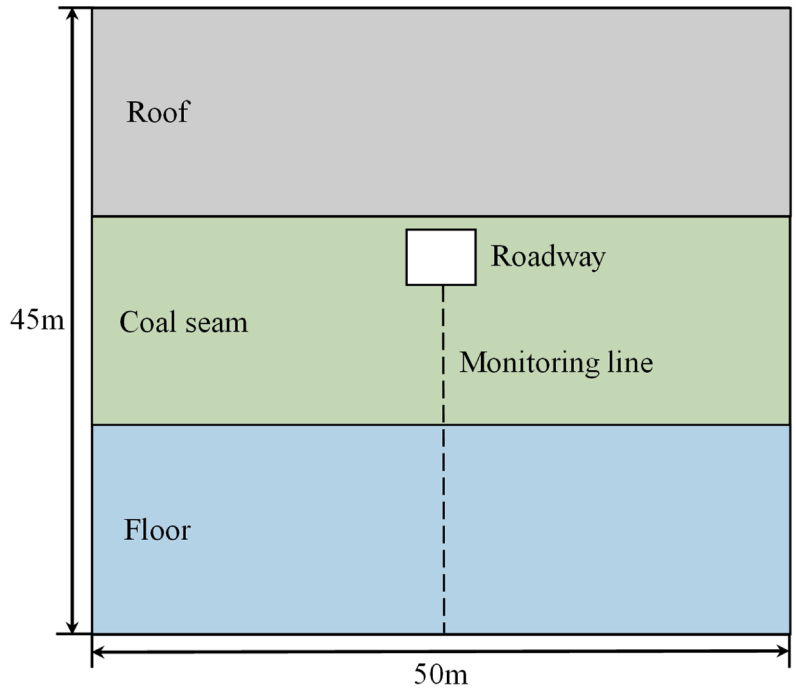


Figure 3. Numerical model of a roadway with retained bottom coal.

To simulate an 800 m burial depth, a vertical stress of 20 MPa was applied at the model top to represent overburden weight, while displacement constraints were imposed on the remaining boundaries. The lateral pressure coefficient was set to 1.5. To reduce the influence of material parameter differences on the simulation results, the roof and floor strata were assigned identical mechanical properties. The coal seam and roof and floor strata were represented using the Mohr–Coulomb constitutive model, and the physical and mechanical parameters are listed in Table 1. All model dimensions, boundary conditions, and material properties were held constant except for bottom coal thickness, allowing its influence on floor horizontal stress, elastic strain energy density, and rockburst instability tendency to be isolated.

Table 1. Physical and mechanical parameters of the coal seam and roof and floor strata [33–35].

Rock Stratum	Density ($Kg.m^{-3}$)	Elastic Modulus (GPa)	Poisson's Ratio	Cohesion (MPa)	Internal Friction Angle (°)	Tensile Strength (MPa)
Roof	2700	2.30	0.25	3.98	40	2.34
Coal seam	1300	1.20	0.32	1.80	35	1.20
Floor	2700	2.30	0.25	3.98	40	2.34

After the initial stress field reached equilibrium, the roadway was excavated and the model was solved again to a new static equilibrium state. The horizontal stress, elastic strain

energy density, and their corresponding peak locations were then extracted along the vertical monitoring line beneath the roadway center for subsequent analysis. The same calculation procedure was adopted for all bottom coal thickness cases to ensure consistent comparison.

To evaluate the influence of mesh size on the numerical simulation results, a representative case with a bottom coal thickness of 4 m was selected. Numerical models with global mesh sizes of 1.0 m, 0.5 m, and 0.25 m were established. Based on the model with a mesh size of 0.25 m, local mesh refinement to 0.125 m was further performed within a range of 5 m on both sides of the roadway and 10 m beneath the roadway floor. The peak horizontal stress, peak elastic strain energy density, and their corresponding locations were extracted from the four mesh configurations as quantitative evaluation indicators to assess the influence of mesh size on the monitoring results. The calculation results are presented in Table 2.

Table 2. Results of mesh sensitivity analysis [34].

Mesh Size (m)	Number of Elements	Peak Horizontal Stress (MPa)	Peak Horizontal Stress Location (m)	Peak Elastic Strain Energy Density ($kJ \cdot m^{-3}$)	Peak Elastic Strain Energy Density Location (m)
1.0	45,000	40.96	3.57	599.22	3.06
0.5	360,000	44.39	3.57	670.98	3.06
0.25	2,880,000	46.05	3.57	731.38	3.57
0.125	4,576,000	49.87	4.08	785.27	3.57

As shown in Table 2, both the peak horizontal stress and peak elastic strain energy density generally increase with mesh refinement. When the global mesh size was reduced from 1.0 m to 0.5 m, the peak horizontal stress and peak elastic strain energy density increased by approximately 8.37% and 11.98%, respectively, while the peak locations of both indicators remained unchanged. When the mesh size was further reduced from 0.5 m to 0.25 m, the peak horizontal stress increased by approximately 3.74%, with its peak location remaining at 3.57 m below the roadway floor. The peak elastic strain energy density increased by approximately 9.00%, and its peak location shifted from 3.06 m to 3.57 m. Following local mesh refinement, the peak horizontal stress increased from 46.05 MPa to 49.87 MPa, representing an increase of approximately 8.30%, and its peak location shifted from 3.57 m to 4.08 m below the roadway floor. The peak elastic strain energy density increased from 731.38 $kJ \cdot m^{-3}$ to 785.27 $kJ \cdot m^{-3}$, representing an increase of approximately 7.37%, while its peak location remained at 3.57 m.

These results indicate that the peak values of stress and elastic strain energy density, as well as their locations, exhibit a certain degree of mesh sensitivity. However, this study primarily focuses on the overall spatial distributions and relative variations in stress and energy in the composite floor under different bottom-coal thickness conditions, thereby investigating the evolution of its load-bearing–energy-storage state, rather than relying entirely on the absolute values or precise locations of local peaks. Considering the number of elements, computational accuracy, and computational efficiency, the global mesh size of 0.5 m was considered adequate for comparative analysis across multiple cases. Therefore, this mesh size was adopted for the subsequent numerical simulations.

3.2. Evolution of Floor Load-Bearing and Energy-Storage Characteristics and Rockburst Instability Tendency

Floor rockburst instability tendency is controlled not only by the instability resistance of the bottom coal–floor composite structure but also by stress transfer and elastic strain energy accumulation within the coal-rock mass. Accordingly, this section analyzes the

evolution of floor load-bearing and energy-storage characteristics and rockburst instability tendency from the perspectives of horizontal stress, elastic strain energy density, and their relative changes.

3.2.1. Evolution of Horizontal Stress and Transition of the Main Load-Bearing Body

Horizontal stress is an important driving force for floor extrusion and instability. Figure 4 presents the spatial distribution of floor horizontal stress under different bottom coal thicknesses, the corresponding horizontal-stress profiles along the monitoring line beneath the roadway floor, and the evolution of peak horizontal stress with bottom coal thickness.

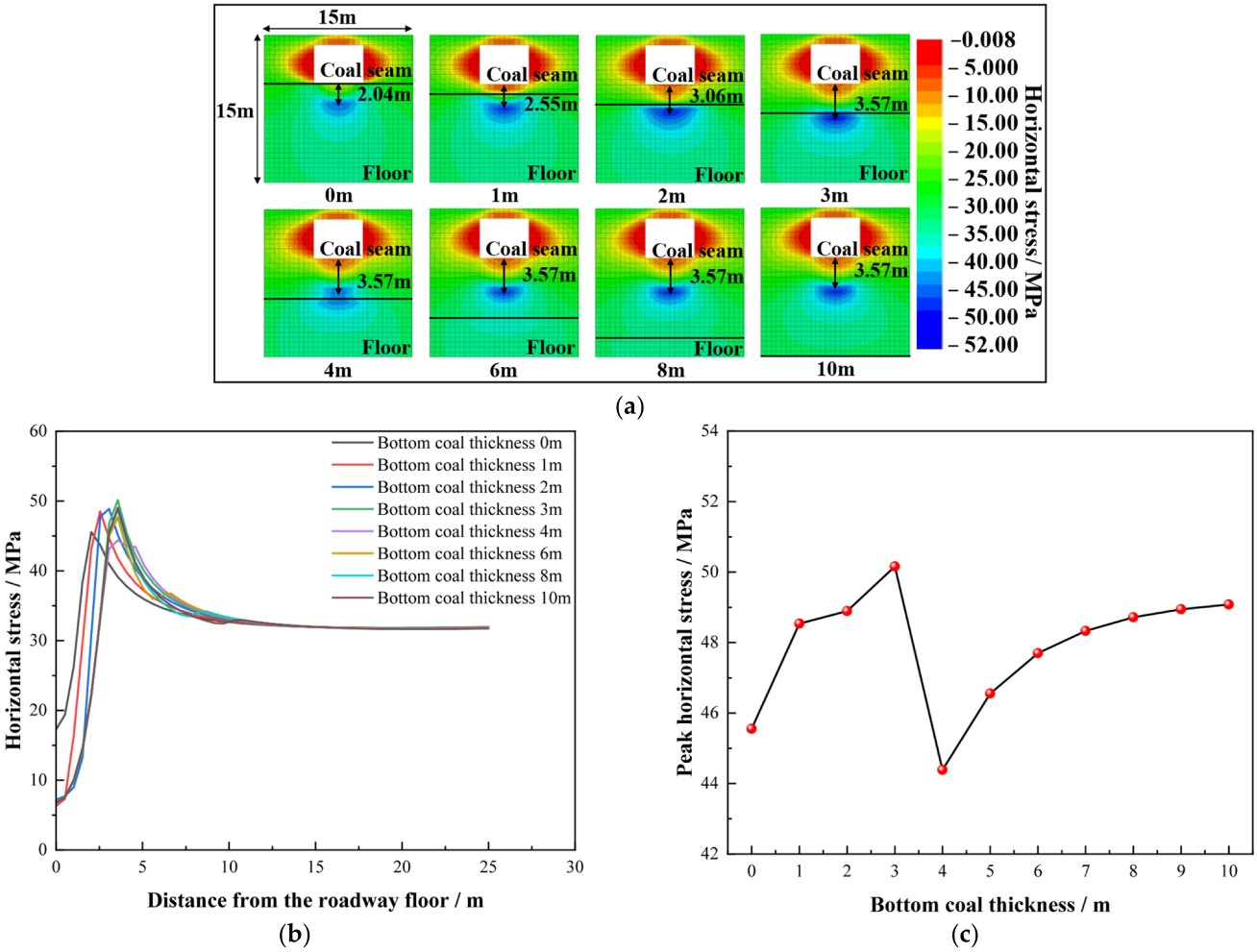


Figure 4. Spatial distribution, monitoring-line profiles, and peak evolution of floor horizontal stress under different bottom coal thicknesses: (**a**) horizontal-stress contours; (**b**) horizontal-stress profiles along the monitoring line; (**c**) variation in peak horizontal stress with bottom coal thickness.

With increasing bottom coal thickness, the peak horizontal stress exhibits a non-monotonic pattern characterized by a rapid increase, a stagewise decrease, and slow recovery followed by stabilization. Without bottom coal, the peak horizontal stress is approximately 45.55 MPa and occurs about 2.04 m below the roadway floor. At a bottom coal thickness of 3 m, the peak rapidly increases to 50.16 MPa and migrates downward to about 3.57 m. At 4 m, the peak decreases to 44.39 MPa; with further thickening to 5–10 m, it gradually recovers and ultimately stabilizes at approximately 49.08 MPa, while the peak position remains near 3.57 m below the roadway floor.

These results indicate that bottom coal thickness changes the stress-transfer path and the principal load-bearing body within the roadway floor. When the bottom coal is thin, its overall bearing capacity is limited, and the shallow bottom coal readily deforms after roadway excavation. Stress is consequently transferred to the stiffer underlying floor strata, which become the main load-bearing body; the stress concentration therefore migrates downward and the peak horizontal stress increases. At a bottom coal thickness of approximately 4 m, the bottom coal develops a certain bearing capacity and the floor begins to transition from floor strata-dominated bearing to composite bearing by the bottom coal and underlying strata. Owing to the pronounced mechanical contrast between coal and floor rock, stress is redistributed within the composite floor and the degree of stress concentration decreases temporarily. The reduction in peak horizontal stress does not imply a lower rockburst instability tendency; rather, it reflects a transition in the load-bearing structure. With further increases in bottom coal thickness, the underlying floor strata move progressively away from the main excavation-disturbance zone, the stress concentration zone shifts into the bottom coal, and thick bottom coal becomes the principal load-bearing body. The peak horizontal stress then recovers slowly and tends to stabilize.

Therefore, the non-monotonic evolution of horizontal stress with bottom coal thickness essentially reflects a progressive transition of the dominant load-bearing body from the floor strata to the bottom coal–floor composite structure, and finally to thick bottom coal. Differences in the mechanical properties and spatial configuration of the coal and rock media govern the floor stress-transfer path, degree of stress concentration, and migration of the peak-stress position.

3.2.2. Evolution of Elastic Strain Energy and Migration of Energy-Storage Zones

Evolution Characteristics of Elastic Strain Energy and Migration of Energy-Storage Zones

Rockburst instability is closely associated with the accumulation and rapid release of elastic strain energy in the coal-rock mass. To characterize the energy-storage response of the roadway floor under different bottom coal thicknesses, elastic strain energy density is used to represent the elastic energy stored in the coal-rock mass under the current stress state and is calculated as:

$$U_e = \frac{\left[\sigma_1^2 + \sigma_2^2 + \sigma_3^2 - 2\nu(\sigma_1\sigma_2 + \sigma_2\sigma_3 + \sigma_1\sigma_3)\right]}{2E} \quad (8)$$

where U_e is the elastic strain energy density of the coal-rock mass, J·m^{-3}; σ_1, σ_2, and σ_3 are the maximum, intermediate, and minimum principal stresses, respectively, Pa; ν is Poisson's ratio; and E is the elastic modulus, Pa.

Based on Equation (8), the elastic strain energy density of the roadway floor was calculated using FISH. The core FISH function used for the calculation is provided in Appendix A for reproducibility. Figure 5 presents the spatial distribution of floor elastic strain energy density under different bottom coal thicknesses, the corresponding elastic strain energy density profiles along the monitoring line beneath the roadway floor, and the evolution of peak elastic strain energy density with bottom coal thickness.

The peak elastic strain energy density generally increases with bottom coal thickness and exhibits a staged pattern of slow increase, rapid growth, and gradual stabilization. Without bottom coal, the peak value is approximately 458.12 kJ·m^{-3} and occurs about 2.04 m below the roadway floor. At a bottom coal thickness of 2 m, it increases slowly to 512.35 kJ·m^{-3} while the peak position migrates downward. At 3–5 m, the peak value increases rapidly and reaches approximately 748.27 kJ·m^{-3}. At 6–10 m, the elastic strain energy density remains high, but its growth rate decreases, while the peak position remains essentially stable at approximately 3.57 m below the roadway floor.

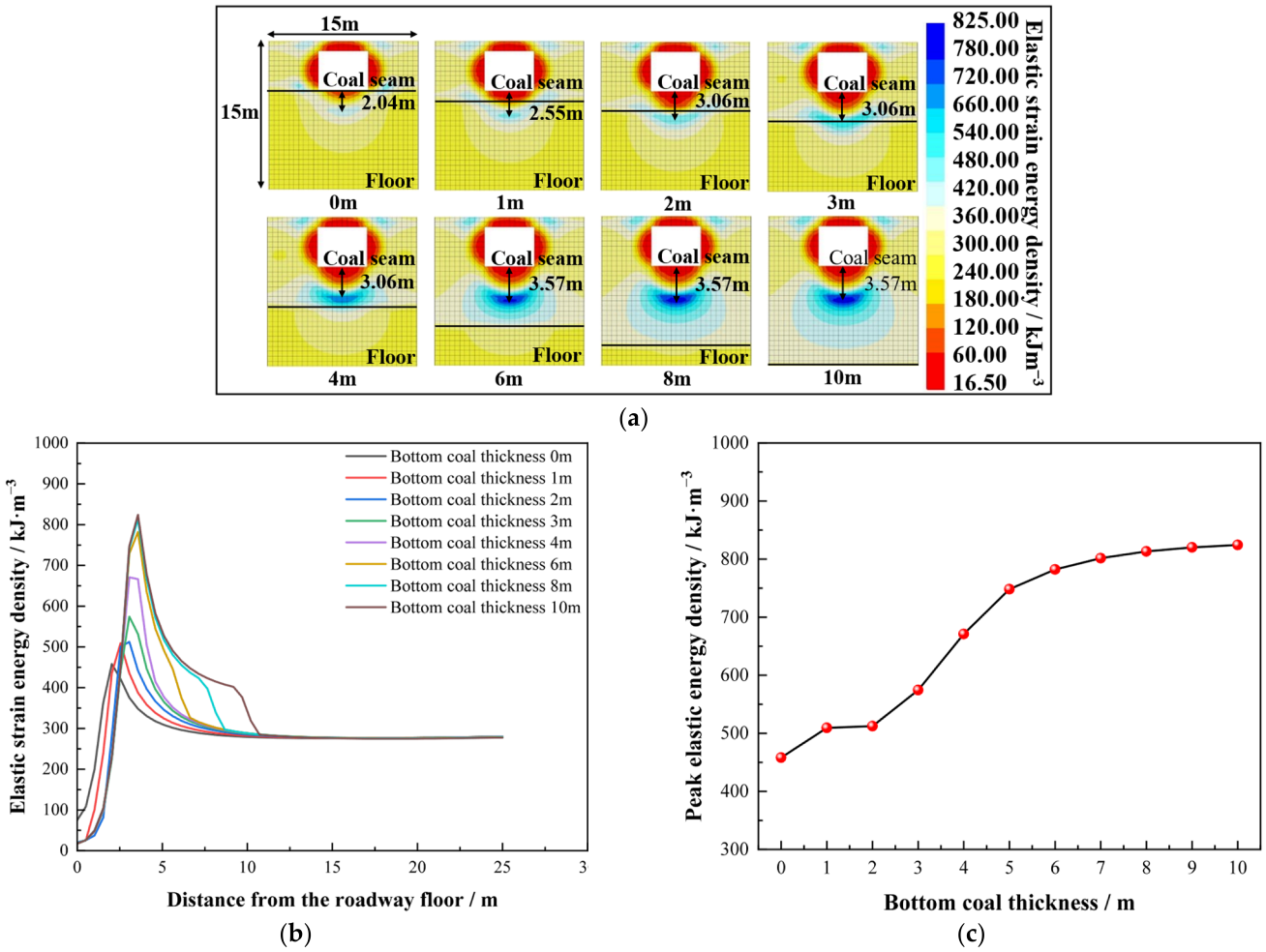


Figure 5. Spatial distribution, monitoring-line profiles, and peak evolution of floor elastic strain energy density under different bottom coal thicknesses: (**a**) elastic strain energy density contours; (**b**) elastic strain energy density profiles along the monitoring line; (**c**) variation in peak elastic strain energy density with bottom coal thickness.

Under thin-bottom-coal conditions, the floor strata still carry most of the load and dominate the overall energy-storage state; therefore, the peak elastic strain energy density increases only slowly with increasing bottom coal thickness. As bottom coal thickness further increases, the bottom coal gradually participates in the energy-storage process of the composite floor. Due to the significant differences in elastic modulus and deformation response between coal and floor strata, stress and deformation within the composite floor are redistributed, causing elastic strain energy to progressively concentrate in the bottom coal and adjacent zones, and the peak elastic strain energy density enters a rapid growth stage. Notably, under some intermediate bottom coal thickness conditions, the peak horizontal stress location and peak elastic strain energy density location do not completely coincide, indicating that the maximum stress concentration zone and maximum elastic energy accumulation zone may be spatially decoupled. This suggests that during the coal-rock composite load-bearing stage, horizontal stress concentration alone cannot fully characterize the floor rockburst instability tendency, and the energy-storage level of the coal-rock mass and its spatial distribution should also be considered. With further increase in bottom coal thickness, thick bottom coal gradually becomes the dominant load-bearing and energy-storage zone of the floor. The stress concentration zone and energy accumulation zone are mainly located within the bottom coal, while the elastic strain energy density remains at a high level and gradually stabilizes.

Overall, with increasing bottom coal thickness, the dominant energy-storage zone of the floor gradually migrates from the floor strata to the adjacent coal-rock composite zone and finally to the interior of thick bottom coal, reflecting the adjustment of the floor energy-storage state caused by changes in the composite structure. The floor structure evolves from a relatively high-stiffness and low-energy-storage rock-dominated structure to a low-stiffness and high-energy-storage coal-dominated structure, resulting in higher elastic energy accumulation in the floor coal-rock mass and providing more favorable energy conditions for floor rockburst instability.

Effects of Material Modulus and Structural Adjustment on Elastic Strain Energy Density

The elastic strain energy density of the composite floor is influenced not only by the stress state but also by the elastic parameters of the materials. Due to the significant difference in elastic modulus between the bottom coal and floor strata, an elastic modulus normalization method was adopted to distinguish the effects of bottom coal material properties and composite structural effects on the evolution of the floor energy-storage state. The normalized elastic strain energy density was calculated as follows:

$$U^{*}_{\mathrm{e},i} = U_{\mathrm{e},i}\frac{E_i}{E_{\mathrm{f}}} \tag{9}$$

where $U^{*}_{\mathrm{e},i}$ is the normalized elastic strain energy density of the i-th computational zone, J·m^{-3}; $U_{\mathrm{e},i}$ is the original elastic strain energy density of the i-th computational zone, J·m^{-3}; E_i is the elastic modulus of the material to which the i-th computational zone belongs, GPa; and E_{f} is the elastic modulus of the floor strata, GPa.

The original elastic strain energy density reflects the elastic energy-storage response resulting from the combined effects of the actual material parameters and the current stress state. Using the elastic modulus of the floor strata as a uniform reference value, the normalization procedure in Equation (9) eliminates the inverse elastic modulus term in Equation (8), thereby reducing the direct influence of differences in elastic modulus among materials on the energy response. Specifically, the original elastic strain energy density of each computational zone is normalized individually, after which the peak normalized elastic strain energy density is extracted for comparison among cases with different bottom coal thicknesses. This procedure helps analyze the direct contribution of the elastic modulus of the material to the energy response.

The evolution characteristics of the peak elastic strain energy density before and after normalization under different bottom coal thicknesses are shown in Figure 6. As shown in Figure 6, the original peak elastic strain energy density generally increases continuously with increasing bottom coal thickness, indicating that the energy-storage level of the actual bottom coal–floor composite structure increases with increasing bottom coal thickness. After normalization, the influence of the difference in elastic modulus between coal and rock materials is weakened. The increasing trend of peak elastic strain energy density becomes significantly less pronounced and gradually stabilizes when the bottom coal thickness exceeds 5 m, indicating that the increase in original elastic strain energy density contains a significant contribution from the material effect of low elastic modulus coal.

Therefore, the increase in elastic strain energy density caused by increasing bottom coal thickness is the result of the combined effects of material and structural factors. On the one hand, increasing bottom coal thickness reduces the structural stability of the composite floor; on the other hand, bottom coal increases the energy-storage level of the composite floor under the actual stress state. The coexistence of a low-stability structure and a high energy-storage state promotes an increase in the instability tendency of the floor.

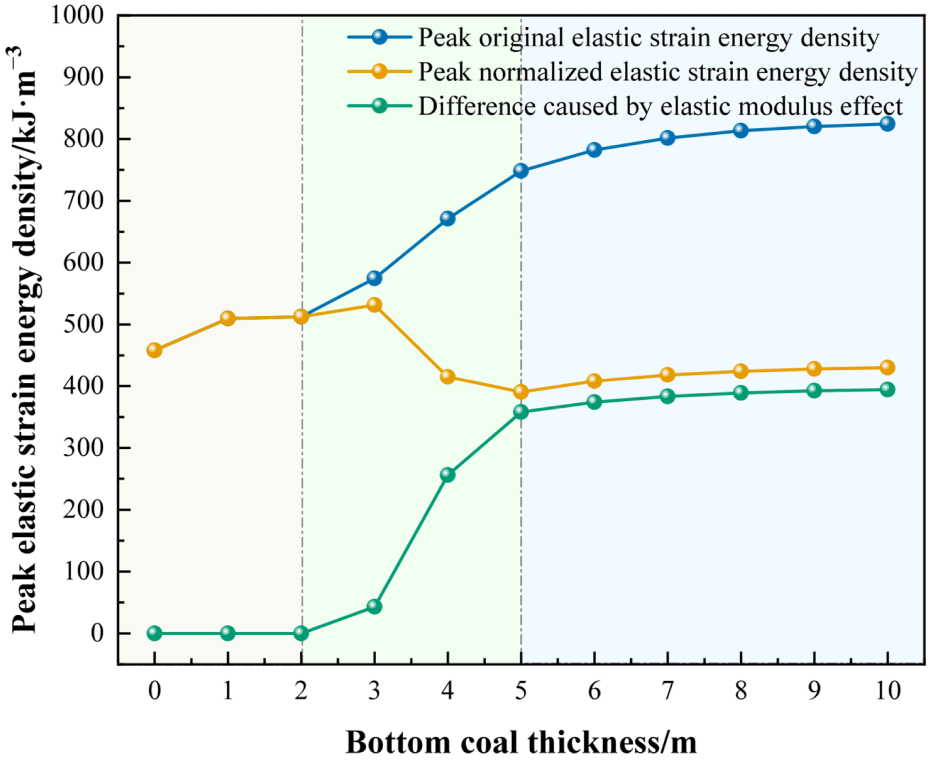


Figure 6. Evolution of peak elastic strain energy density before and after normalization under different bottom coal thicknesses.

3.2.3. Energy-Stress Index *K* and Evolution of the Load-Bearing and Energy-Storage States

The preceding analysis shows that bottom coal thickness affects the peak horizontal stress and peak elastic strain energy density in different ways. Therefore, evaluating the floor instability tendency under different bottom coal thickness conditions using either stress or energy alone has certain limitations. An energy-stress index *K* is introduced, which is defined as the ratio of peak elastic strain energy density to peak horizontal stress. The index is mainly used to characterize the relative variation in the energy-storage response with respect to the load-bearing level of the floor coal-rock mass under different bottom coal thickness conditions, thereby reflecting the evolution of the load-bearing and energy-storage states of the floor. It should be noted that the peak horizontal stress and peak elastic strain energy density may occur at different spatial locations under some conditions. Therefore, *K* does not represent the energy-storage efficiency at a specific location, but rather reflects the relative evolution of the overall load-bearing and energy-storage state of the composite floor under different conditions.

$$K = \frac{U_{\max}}{\sigma_{\max}} \tag{10}$$

where $U_{\max}$ is the peak elastic strain energy density stored in the coal-rock mass, J·m^{-3}; and $\sigma_{\max}$ is the peak horizontal stress of the coal-rock mass, Pa.

A smaller *K* value indicates that the energy-storage response corresponding to the unit bearing level of the coal-rock mass is relatively weak, and the floor behavior is mainly controlled by load bearing. An increase in *K* indicates a stronger energy-storage response relative to the load-bearing level and, when considered together with the reduction in structural stiffness and the spatial concentration of stress and energy, may indicate an increase in floor rockburst instability tendency.

The evolution of *K* under different bottom coal thicknesses is shown in Figure 7. As shown in Figure 7, *K* increases monotonically with bottom coal thickness and exhibits a staged evolution characterized by slow growth, rapid surge, and stabilization. For bottom

coal thicknesses of 0–2 m, *K* increases only slightly from 0.010 to 0.0105, indicating a state dominated by load bearing in the floor strata with a relatively weak energy-storage response. At 2–5 m, *K* increases rapidly from 0.0105 to 0.0161, with the most pronounced increase occurring at approximately 3–4 m. During this stage, the peak horizontal stress undergoes significant redistribution, while the elastic strain energy density continues to increase rapidly, indicating that the energy-storage response increases more rapidly than the load-bearing response. As bottom coal gradually participates in the load-bearing process of the floor, the floor evolves from a floor strata-dominated load-bearing state toward a composite load-bearing and energy-storage state of the bottom coal–floor structure. The rapid increase in *K* reflects a rapid adjustment of the relationship between floor load bearing and energy storage and represents the critical stage of floor stability evolution induced by increasing bottom coal thickness. At 5–10 m, *K* increases slowly from 0.0161 to 0.0168 and gradually approaches a plateau. Thick bottom coal gradually becomes the dominant region controlling the load-bearing and energy-storage state of the floor, while both horizontal stress and elastic strain energy density remain at relatively high levels. The floor develops into a low-stiffness coal-rock structure-controlled state with a high energy-storage response. Although *K* no longer increases rapidly, it remains at a relatively high level, indicating that the floor remains in a high-stress and high energy-storage response state, with a relatively high tendency toward rockburst instability.

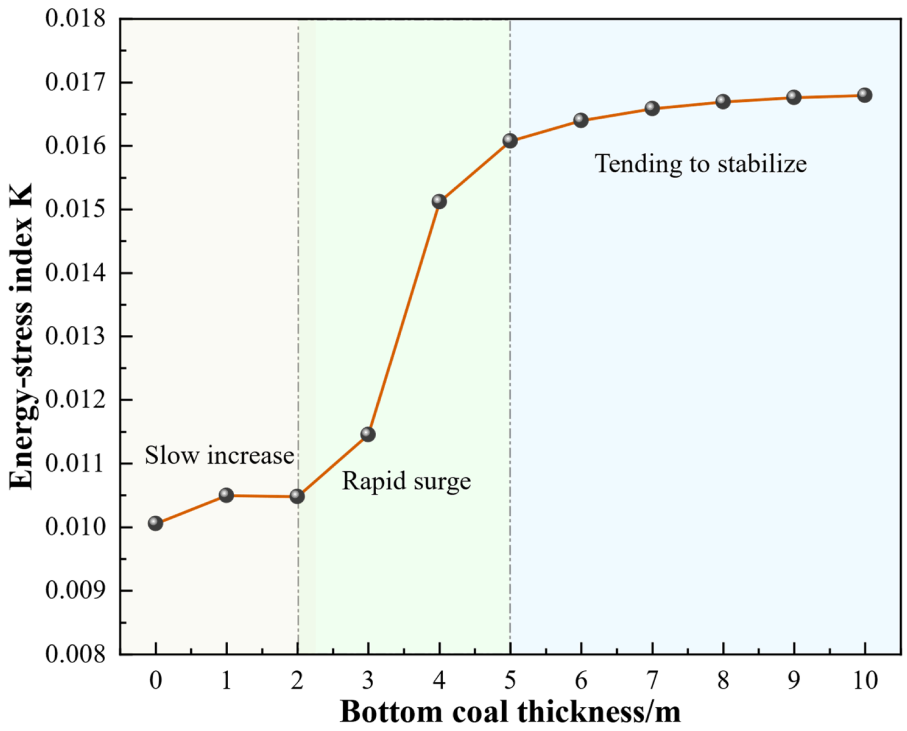


Figure 7. Evolution of the floor energy-stress index *K* under different bottom coal thicknesses.

Overall, the staged evolution of *K* reflects the evolution of the load-bearing and energy-storage relationship of the composite floor with increasing bottom coal thickness. In the thin-bottom-coal stage, load bearing is mainly controlled by the floor strata and energy storage is relatively limited. At intermediate bottom coal thicknesses, the load-bearing and energy-storage states undergo rapid adjustment. Under thick-bottom-coal conditions, a load-bearing and energy-storage state dominated by bottom coal is gradually formed. Therefore, the increase in bottom coal thickness promotes the adjustment of the load-bearing and energy-storage states, which is an important factor contributing to the enhancement of floor rockburst instability tendency.

Taken together, the theoretical analysis in Section 2 and the numerical results in Section 3 demonstrate that bottom coal thickness affects the floor rockburst instability tendency through both structural effects and load-bearing and energy-storage effects. With increasing bottom coal thickness, the equivalent flexural stiffness of the bottom coal–floor composite structure decreases, weakening its resistance to deformation and instability. Meanwhile, differences in elastic modulus between coal and rock materials and structural adjustment jointly influence the load-bearing and energy-storage state of the floor, resulting in enhanced elastic strain energy accumulation. Therefore, the increase in floor rockburst instability tendency is jointly governed by reduced structural resistance and the adjustment of the load-bearing and energy-storage state.

4. Optimization of Floor Borehole Pressure-Relief Horizons in Roadways with Retained Bottom Coal

Increasing bottom coal thickness not only changes the degree of stress concentration in the floor but also causes the dominant load-bearing and energy-storage bodies to migrate. Consequently, the main controlling horizon of floor rockburst instability tendency varies with bottom coal thickness. Floor borehole pressure relief is a common engineering measure for controlling floor rockbursts. Rather than adopting a uniform borehole depth, the borehole-weakened zone should be matched to the main floor load-bearing and energy-storage zone so that targeted pressure relief can be achieved. Accordingly, the following sections investigate borehole pressure-relief responses and reasonable pressure-relief horizons under different bottom coal thicknesses.

4.1. Numerical Model and Simulation Scheme for Floor Borehole Pressure Relief

To investigate how borehole vertical depth regulates the floor load-bearing and energy-storage state under different bottom coal thicknesses, a floor borehole pressure-relief model was established, as shown in Figure 8.

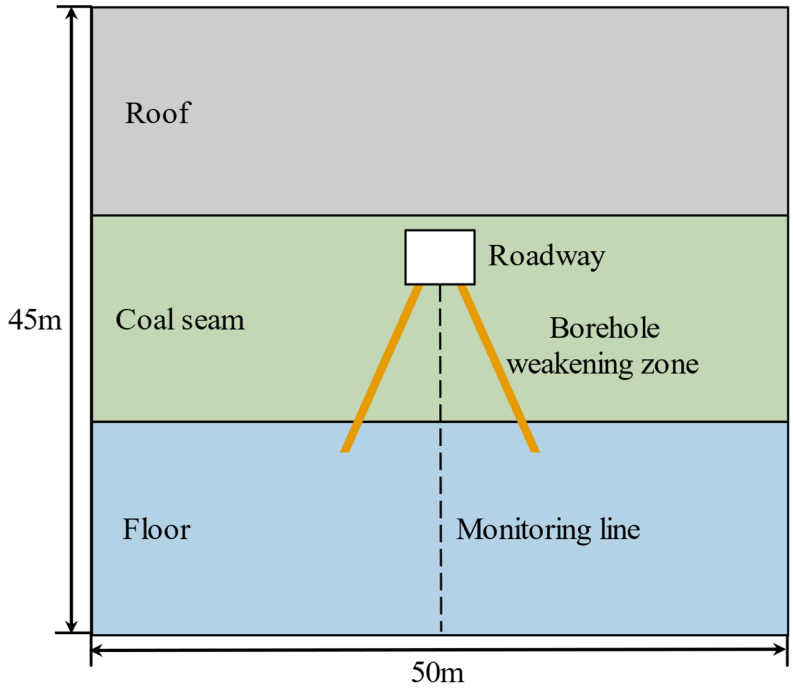


Figure 8. Numerical model for floor borehole pressure relief. The yellow lines delineate the borehole weakening zones, and the dashed line indicates the monitoring line.

In engineering practice, drilling causes fracturing and strength degradation around the borehole, and the disturbance zones of adjacent boreholes may overlap to form a relatively continuous weakened zone. Accordingly, a prefabricated weakened band was used to equivalently represent the overall pressure-relief effect of a borehole group. Referring to commonly used field parameters, the borehole diameter was set to 150 mm, spacing to 1.0 m, and the angle between the borehole axis and roadway floor to 65°. A 0.5 m wide rectangular weakened band was arranged along the 65° direction at a distance of 1.0 m from the roadway rib, and the mechanical properties of the coal-rock mass within the band were reduced to represent the fractured weakened zone produced by borehole pressure relief [35]. Due to the inclination angle between the weakened zone and the coal-rock strata, local mesh refinement was applied to the weakened zone based on the global mesh size of 0.5 m. The model boundary conditions, constitutive models, and other settings were consistent with those in Section 3.

Based on the evolution of floor load-bearing and energy-storage states, bottom coal thicknesses of 2, 4, 6, and 8 m were selected as representative cases. The 2 m case represents thin bottom coal, the 4 m case represents a composite load-bearing and energy-storage state of the bottom coal–floor structure, and the 6 and 8 m cases represent thick-bottom-coal-dominated states. Borehole vertical depths ranging from 0 to 12 m were simulated at 0.5 m intervals. The effects of borehole vertical depth on horizontal stress, elastic strain energy density, energy-stress index K, and floor deformation were analyzed to clarify the regulation mechanism of borehole pressure relief on the floor load-bearing and energy-storage state and to determine reasonable pressure-relief horizons.

To verify the stability of the borehole pressure-relief evaluation results with respect to the selection of weakening parameters, a sensitivity analysis under different weakening degrees was further conducted. While keeping the borehole arrangement and calculation scheme unchanged, different weakening degrees (70%, 80%, and 90% reductions) were assigned to the mechanical parameters of the coal-rock mass in the weakened zone, including elastic modulus, cohesion, and tensile strength. Meanwhile, considering the reduction in shear bearing capacity caused by borehole disturbance, the frictional parameters were weakened accordingly. The variations in the floor load-bearing and energy-storage responses under different weakening degrees were then compared and analyzed.

The simulation results show that variations in weakening degree mainly affect the magnitude of changes in horizontal stress, elastic strain energy density, and deformation response after borehole pressure relief. However, the overall pressure-relief response characteristics and reasonable pressure-relief horizons remain basically unchanged under different bottom coal thickness conditions. This indicates that the optimization results of the borehole horizons obtained in this study do not depend on a single weakening parameter selection and exhibit good stability. Therefore, the subsequent analyses adopted the scheme with a 90% reduction in the mechanical parameters of the coal-rock mass within the weakened zone. The roof parameters remained unchanged. When the weakened zone crossed different coal-rock strata, the corresponding material parameters were weakened according to the same principle. The specific mechanical parameters are listed in Table 3.

Table 3. Physical and mechanical parameters of the roof strata and the weakened coal and floor strata.

Rock Stratum	Density ($Kg.m^{-3}$)	Elastic Modulus (GPa)	Poisson's Ratio	Cohesion (MPa)	Internal Friction Angle (°)	Tensile Strength (MPa)
Roof	2700	2.30	0.25	3.98	40	2.34
Coal seam	1300	0.12	0.32	0.18	18	0.12
Floor	2700	0.23	0.25	0.398	20	0.234

4.2. Load-Bearing and Energy-Storage Response of the Floor to Borehole Pressure Relief

Figure 9 shows the variations in floor horizontal stress and elastic strain energy density with borehole vertical depth under different bottom coal thicknesses. Overall, both indices generally decrease as borehole vertical depth increases, although their responses are not fully synchronous.

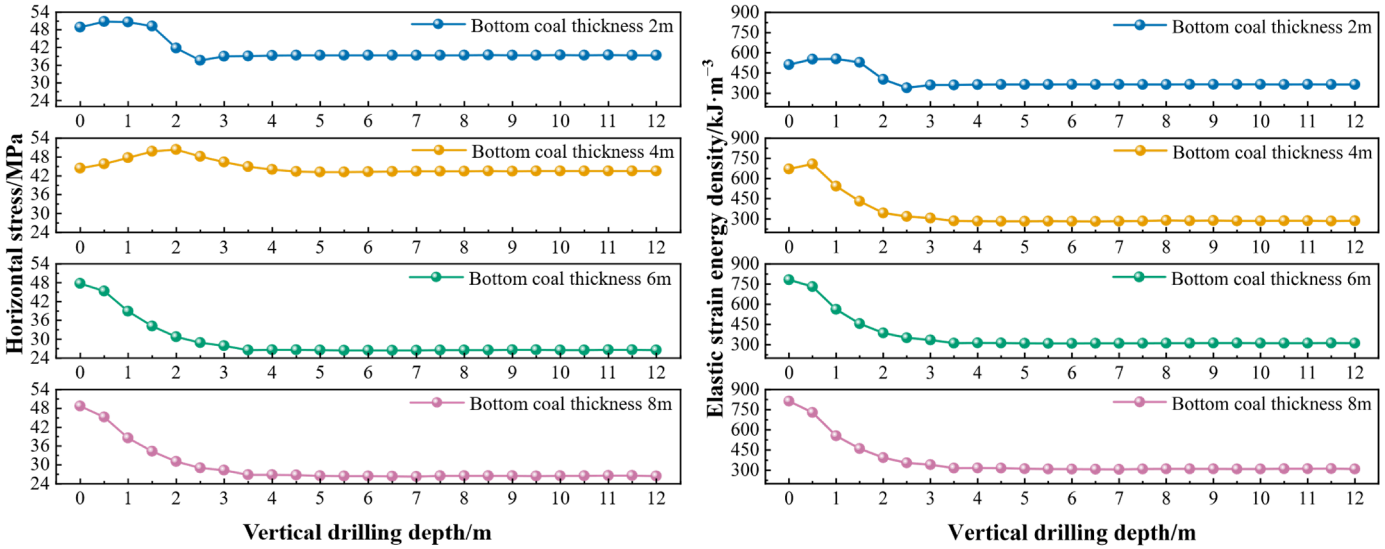


Figure 9. Evolution of horizontal stress and elastic strain energy density with borehole vertical depth under different bottom coal thicknesses: (**a**) horizontal stress; (**b**) elastic strain energy density.

At a bottom coal thickness of 2 m, horizontal stress and elastic strain energy density both exhibit an initial increase followed by a decrease and eventual stabilization. When the borehole vertical depth is less than 1.5 m, the borehole mainly affects the shallow thin-bottom-coal zone and has not yet entered the principal load-bearing and energy-storage zone in the underlying floor strata. Local pressure-relief disturbance may therefore redistribute stress and energy toward deeper intact rock, causing both indices to increase relative to the case without pressure relief. As the borehole deepens, the weakened zone progressively enters the main load-bearing and energy-storage zone in the floor strata, disrupting the original continuous load-bearing structure and causing horizontal stress and elastic strain energy density to decrease markedly. When the borehole vertical depth exceeds 3.0 m, both indices approach stable values, indicating that the main load-bearing and energy-storage zone has been effectively weakened. Thus, under thin-bottom-coal conditions, pressure relief is characterized by an initial disturbance followed by effective relief; a pronounced pressure-relief effect is obtained only after the borehole passes through the bottom coal and enters the principal load-bearing and energy-storage zone of the underlying floor strata.

At a bottom coal thickness of 4 m, horizontal stress and elastic strain energy density respond asynchronously to increasing borehole vertical depth. The elastic strain energy density decreases first and continuously, whereas the horizontal stress initially increases and then decreases; both tend to stabilize once the borehole vertical depth exceeds approximately 4.0 m. Under the 4 m condition, the floor is in a composite load-bearing and energy-storage state of the bottom coal–floor structure. Elastic strain energy is concentrated mainly within the bottom coal, while the principal horizontal stress concentration zone lies closer to the coal-rock composite region. As the borehole deepens, the weakened zone first acts on the bottom coal energy-storage zone, promoting preferential energy release. Only after the

borehole extends further into the coal-rock composite load-bearing zone is the continuous load-bearing structure substantially weakened and the horizontal stress reduced. Thus, pressure relief under the 4 m bottom coal condition is characterized by energy release followed by load redistribution, and an effective design should account for both the bottom coal energy-storage zone and the coal-rock composite load-bearing zone.

At bottom coal thicknesses of 6 and 8 m, horizontal stress and elastic strain energy density exhibit similar trends: both decrease markedly with increasing borehole vertical depth and gradually stabilize once the depth exceeds approximately 4.0 m. At this stage, thick bottom coal has become the principal load-bearing and energy-storage body, and both the stress concentration and energy accumulation zones are located mainly within the bottom coal. As the borehole deepens, the weakened zone simultaneously weakens the continuous load-bearing structure and the high-energy accumulation zone, resulting in relatively synchronous decreases in horizontal stress and elastic strain energy density. Once the borehole extends beyond the main high-load-bearing and high-energy-storage zone, further increases in depth produce only limited improvement. Therefore, thick-bottom-coal conditions are characterized by simultaneous regulation of load bearing and energy storage, with the principal pressure-relief target located within the high-stress, high-energy-storage zone of the thick bottom coal.

In summary, under thin-bottom-coal conditions, the borehole must enter the principal load-bearing and energy-storage zone of the underlying floor strata before effective pressure relief occurs. At intermediate bottom coal thicknesses, the floor instability tendency is jointly controlled by the bottom coal energy-storage zone and the coal-rock composite load-bearing zone, and the borehole should cover both regions. Under thick-bottom-coal conditions, the main load-bearing and energy-storage zones are concentrated within the bottom coal, and the pressure-relief effect approaches saturation once the borehole penetrates this zone. These results demonstrate that pressure-relief effectiveness is governed primarily by whether the weakened zone covers the principal load-bearing and energy-storage region, rather than increasing linearly with borehole depth.

4.3. Determination of Reasonable Borehole Pressure-Relief Horizons

Horizontal stress and elastic strain energy density reflect how borehole pressure relief regulates the floor load-bearing and energy-storage state, but their responses to borehole vertical depth are not fully synchronous. A single stress or energy index is therefore insufficient for accurately identifying a reasonable pressure-relief horizon. The energy-stress index K and floor deformation are consequently used in combination. K characterizes the relative variation between the floor load-bearing level and energy-storage response under different borehole vertical depths, while floor deformation indicates whether borehole-induced deformation release has become sufficient. A marked decrease and subsequent stabilization of K, together with a transition of floor deformation from growth to stabilization and only minor changes in both indices with further borehole deepening, indicates that pressure relief has effectively improved the floor load-bearing and energy-storage state and that the pressure-relief effect is approaching saturation.

The evolution of K and floor deformation with borehole vertical depth is shown in Figure 10. For a bottom coal thickness of 2 m, K is slightly higher than that in the state without pressure relief when the borehole vertical depth is less than 1.5 m, while floor deformation continues to increase, indicating that shallow boreholes have not yet entered the principal load-bearing and energy-storage zone and provide little pressure relief. At depths of 1.5–2.5 m, K begins to decrease, indicating that the borehole is entering an effective pressure-relief range, although floor deformation is still increasing. When the depth exceeds

3.0 m, both K and floor deformation approach plateau values, and further deepening produces little additional improvement.

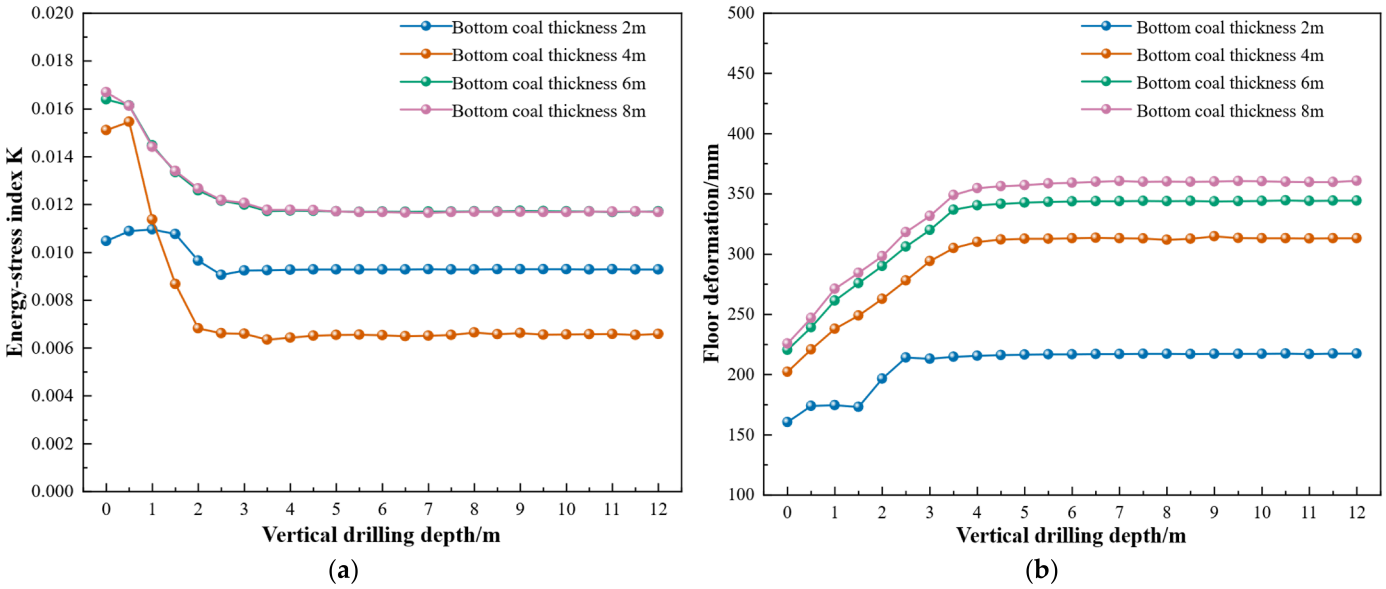


Figure 10. Evolution of energy-stress index K and floor deformation with borehole vertical depth under different bottom coal thicknesses: (**a**) energy-stress index K; (**b**) floor deformation.

At a bottom coal thickness of 4 m, K decreases continuously as the borehole vertical depth increases from 0.5 to 3.5 m, indicating progressive weakening of the energy-storage response corresponding to the unit load-bearing level and continuous improvement of the load-bearing and energy-storage state. However, floor deformation continues to increase, showing that borehole-induced deformation release has not yet stabilized. When the borehole vertical depth exceeds 4.0 m, both K and floor deformation gradually stabilize, indicating that the weakened zone has essentially covered the principal bottom coal energy-storage zone and the coal-rock composite load-bearing zone. Further borehole deepening provides only limited additional pressure relief.

At bottom coal thicknesses of 6 and 8 m, K decreases and floor deformation increases progressively as the borehole deepens, indicating that the continuous load-bearing structure and energy-storage state within the thick bottom coal are continuously weakened within the thick bottom coal. Once the borehole vertical depth exceeds 4.0 m, both indices gradually stabilize, indicating that the borehole has essentially covered the principal high-load-bearing and high-energy-storage zone within the thick bottom coal and that further deepening yields little additional benefit.

To further quantitatively determine the stabilization stage of the borehole pressure-relief effect, the variation rates of the energy-stress index K and floor deformation are adopted to evaluate the regulation effect caused by further increasing borehole depth. The variation rates η_K and η_D are defined as follows:

$$\eta_K = \frac{|K_{d+0.5} - K_d|}{K_d} \times 100\% \tag{11}$$

$$\eta_D = \frac{|D_{d+0.5} - D_d|}{D_d} \times 100\% \tag{12}$$

where η_K represents the variation rate of the energy-stress index K between adjacent borehole depths; η_D represents the variation rate of floor deformation between adjacent borehole depths; K_d is the energy-stress index K at the current borehole vertical depth d; $K_{d+0.5}$ is

the energy-stress index K after increasing the borehole vertical depth by 0.5 m; D_d is the floor deformation at the current borehole vertical depth d, mm; and $D_{d+0.5}$ is the floor deformation after increasing the borehole vertical depth by 0.5 m, mm.

When the borehole vertical depth is increased by 0.5 m and both η_K and η_D are less than 5%, further increasing the borehole depth is considered to have a limited effect on improving the floor load-bearing and energy-storage state and deformation response, indicating that the pressure-relief effect has entered the stabilization stage. The detailed calculation results are presented in Table 4.

Table 4. Determination of the stabilization stage of floor borehole pressure relief.

Bottom Coal Thickness (m)	Initial Borehole Vertical Depth at Stabilization Stage (m)	Maximum $\lvert\eta_K\rvert$ Within Stabilization Stage (%)	Maximum $\lvert\eta_D\rvert$ Within Stabilization Stage (%)	Determination Result (m)
2.0	3.0	2.21	0.84	3.0–4.0
4.0	4.0	1.42	1.67	4.0–5.0
6.0	4.0	0.17	1.04	4.0–5.0
8.0	4.0	0.51	1.62	4.0–5.0

As shown in Table 4, a distinct stabilization stage of borehole pressure relief exists under different bottom coal thickness conditions. For a bottom coal thickness of 2 m, when the borehole vertical depth reaches 3.0 m, the maximum values of η_K and η_D within the stabilization stage are 2.21% and 0.84%, respectively, both lower than 5%, indicating that the borehole has essentially entered the effective pressure-relief horizon. For a bottom coal thickness of 4 m, when the borehole vertical depth reaches 4.0 m, the maximum values of η_K and η_D are 1.42% and 1.67%, respectively, indicating that further increasing borehole depth has a limited effect on improving the floor load-bearing and energy-storage state. For bottom coal thicknesses of 6 m and 8 m, after the borehole vertical depth reaches 4.0 m, the variation rates of the two indices within the stabilization stage remain relatively small, indicating that the main load-bearing and energy-storage zones within the thick bottom coal have been effectively weakened. These results are consistent with the plateau stage of the K value and floor deformation shown in Figure 10, providing quantitative support for determining reasonable borehole pressure-relief horizons under different bottom coal thickness conditions.

In summary, the reasonable floor borehole pressure-relief horizon varies with bottom coal thickness. For a bottom coal thickness of 2 m, a reasonable borehole vertical depth is 3.0–4.0 m, with a pressure-relief mode of penetrating through the bottom coal into the underlying floor strata. For a bottom coal thickness of 4 m, the reasonable vertical depth is 4.0–5.0 m, corresponding to coordinated pressure relief of the bottom coal and floor strata. For bottom coal thicknesses of 6 and 8 m, the reasonable vertical depth is also 4.0–5.0 m, corresponding to targeted pressure relief within the bottom coal. The reasonable pressure-relief horizons obtained under different bottom coal thicknesses are summarized in Table 5.

These results indicate that floor borehole pressure relief should follow the strategy of identifying the key load-bearing and energy-storage horizon, weakening the corresponding key zone, and adapting borehole depth accordingly. The borehole-affected zone should be matched with the principal load-bearing and energy-storage zone, thereby mitigating the floor instability tendency while avoiding unnecessary increases in borehole depth and drilling work.

Table 5. Borehole pressure-relief horizons determined from numerical simulations under different bottom coal thicknesses.

Bottom Coal Thickness (m)	Load-Bearing and Energy-Storage Characteristics	Main Pressure-Relief Target	Pressure-Relief Mode	Reasonable Borehole Vertical Depth (m)
2.0	Floor strata-dominated load-bearing and energy-storage state	Main load-bearing and energy-storage zone in underlying floor strata	Penetrating through bottom coal into underlying floor strata	3.0–4.0
4.0	Bottom coal–floor composite load-bearing and energy-storage state	Bottom coal energy-storage zone and coal-rock composite load-bearing zone	Coordinated pressure relief of bottom coal and floor strata	4.0–5.0
6.0 and 8.0	Thick-bottom-coal-dominated load-bearing and energy-storage state	High-load-bearing and high-energy-storage zone within thick bottom coal	Targeted pressure relief within bottom coal	4.0–5.0

5. Discussion

5.1. Comparison with Previous Studies

This study investigates the effect of bottom coal thickness from two perspectives: the structural stability of the composite floor and the evolution of its load-bearing–energy-storage state. It reveals the changes in structural stiffness, stress distribution, and energy response associated with variations in bottom coal thickness, as well as their effects on the floor rockburst instability tendency. Tan et al. [19] and Zhang et al. [20] showed that changes in bottom coal thickness affect stress transfer and energy evolution within the coal–rock composite floor. Chen [29] investigated the pressure-relief mechanism of floor boreholes and the optimization of related parameters. The present study is consistent with previous studies in recognizing the influence of bottom coal thickness on floor stability, but differs in its energy evaluation indicators, research scope, and optimization of borehole pressure-relief horizons. The detailed comparison is presented in Table 6.

Table 6. Comparison between the present study and previous studies on bottom coal thickness and floor borehole pressure relief.

Previous Studies	Main Research Conditions and Findings	Relationship to and Differences from the Present Study
Tan et al. [19]	Investigated the mechanical response of the composite floor under different bottom coal thicknesses and coal–rock strength conditions. They found that increasing the strength of the floor rock increased the stress in the coal–rock composite floor while reducing displacement and energy. When the strengths of the floor rock and coal were equal, the increases in floor stress and displacement with varying bottom coal thickness were the smallest, at 34.29% and 33.61%, respectively, while the reduction in elastic strain energy decreased from 14.58% to 9.85%. As bottom coal thickness increased, the stress and displacement of the coal–rock composite floor initially increased and then decreased, whereas the total elastic strain energy gradually decreased.	Both Tan et al. [19] and the present study investigate the effects of bottom coal thickness on the mechanical response and energy response of the composite floor. However, Tan et al. [19] mainly analyzed the overall mechanical response, deformation, and total elastic strain energy of the composite floor, whereas the present study focuses on the structural stability of the composite floor and the spatial evolution of its load-bearing and energy-storage zones based on peak stress and energy indicators.

Table 6. *Cont.*

Previous Studies	Main Research Conditions and Findings	Relationship to and Differences from the Present Study
Zhang et al. [20]	Investigated thin and medium-thickness bottom coal with a thickness below 3 m. They found that elastic energy accumulation in the bottom coal increased with thickness, although the growth rate gradually decreased. The rockburst tendency also increased, exhibiting a threshold at a bottom coal thickness of 2 m; beyond this thickness, further increases in bottom coal thickness had a less pronounced effect on the rockburst tendency.	Both Zhang et al. [20] and the present study investigate the effects of bottom coal thickness on the energy response and instability tendency of the floor. However, the present study considers the influence range of roadway excavation and investigates the evolution of peak stress and peak elastic strain energy density over a bottom coal thickness range of 0–10 m, as well as the migration of the load-bearing and energy-storage zones within the coal–rock composite floor.
Chen [29]	Based on an analysis of the pressure-relief mechanism of floor boreholes, investigated the effects of borehole design parameters on floor pressure relief. The study indicated that favorable floor pressure-relief effects could be achieved with borehole diameters of 140–200 mm, inclination angles of 60–75°, spacings of 1–3 m, and row spacings of 1.4–1.8 m.	Both Chen [29] and the present study focus on floor borehole pressure relief and parameter optimization. However, Chen [29] mainly investigated the effects of borehole diameter, inclination angle, spacing, and row spacing on pressure-relief performance, whereas the present study addresses the selection of borehole pressure-relief horizons under different bottom coal thickness conditions and proposes matching the selected horizons to the key load-bearing and energy-storage zones of the floor.

Regarding the energy response, Tan et al. [19] reported that the total elastic strain energy of the composite floor could decrease with increasing bottom coal thickness. Zhang et al. [20] found that, with the thickness of the floor rock held constant, the elastic strain energy in the bottom coal increased with increasing thickness, although the growth rate gradually decreased and a threshold effect was observed. In contrast, the present study shows an overall increase in peak elastic strain energy density with increasing bottom coal thickness. Previous studies primarily examined changes in the overall energy-storage capacity of the composite floor or bottom coal, reflecting the accumulation of elastic strain energy across the investigated region. The present study uses peak elastic strain energy density to characterize the maximum local energy concentration. These indicators have different physical meanings and are therefore not directly equivalent. The difference in the observed trends reflects the different spatial scales and evaluation indicators used to characterize the energy response of the coal–rock composite structure, rather than a direct contradiction between the findings.

Regarding the research scope and evaluation indicators, the threshold effect at a bottom coal thickness of 2 m reported by Zhang et al. [20] primarily reflects changes in the floor rockburst tendency under the conditions considered in their study. The present study further investigates structural stability, the differential responses of peak stress and peak elastic strain energy density, and the spatial evolution of the principal load-bearing and energy-concentration zones over a bottom coal thickness range of 0–10 m. Therefore, the two studies differ in both research scope and evaluation indicators.

Regarding borehole pressure relief, Chen [29] primarily investigated the effects of geometric parameters, including borehole diameter, inclination angle, spacing, and row

spacing, on pressure-relief performance. The present study further addresses the selection of floor borehole pressure-relief horizons under different bottom coal thickness conditions. The spatial correspondence between the borehole weakened zone and the key load-bearing and energy-storage zones of the floor is used as the basis for optimizing the pressure-relief horizon, with the aim of balancing effective pressure relief and construction workload.

5.2. Physical Meaning and Applicability of the Energy-Stress Index K

The normalization analysis of elastic strain energy density with respect to elastic modulus indicates that the low elastic modulus of the bottom coal makes a significant contribution to the increase in the original peak elastic strain energy density. As the energy–stress index K is defined as the ratio of peak elastic strain energy density to peak horizontal stress, its variation is also affected by the elastic properties of the materials. In addition, K is calculated from numerical simulation results, and its value is also influenced by factors such as model dimensions and boundary conditions. Nevertheless, this study uses K to characterize the relative evolution of the load-bearing and energy-storage states of the composite floor under different bottom coal thickness conditions, reflecting the combined effects of the actual material parameters and stress state. The numerical simulation results show that, for some intermediate bottom coal thicknesses, the peak horizontal stress decreases temporarily, whereas the peak elastic strain energy density continues to increase, indicating a clear difference in their evolution patterns. The participation of bottom coal in load bearing changes the stress and energy distributions within the coal–rock composite structure, as well as its deformation compatibility, leading to spatial migration of the main load-bearing and energy-storage zones. By combining the peak elastic strain energy density and peak horizontal stress, K captures the response characterized by "decreasing stress and increasing energy," thereby revealing significant adjustments in the load-bearing and energy-storage states of the composite floor. Therefore, K is used as an auxiliary indicator to characterize the relative evolution of the load-bearing and energy-storage states among numerical cases with different bottom coal thicknesses and to investigate the influence of bottom coal thickness on the evolution of these states in the composite floor. It is not used as an independent criterion for rockburst risk assessment or as a direct predictor of rockburst risk in the field.

5.3. Model Limitations and Engineering Applicability

Both the theoretical model and numerical model adopted in this study involve appropriate simplifications. In the theoretical analysis, the bottom coal and floor strata are considered as a continuous composite structure, which is mainly used to reveal the influence mechanism of bottom coal thickness on the stiffness and stability of the composite structure. Therefore, interlayer slip, interface weakening, complex nonlinear failure processes, and other factors are not considered.

In the numerical simulation, the Mohr–Coulomb model is adopted to describe stress adjustment, energy accumulation, and deformation response of coal-rock masses after excavation. However, this model has limited capability in representing progressive damage and energy release processes during rockburst occurrence. Therefore, the results primarily reveal the relative evolution of the floor rockburst instability tendency under different bottom coal thickness conditions and should not be directly interpreted as the probability of dynamic hazards occurring in the field. The proposed reasonable borehole pressure-relief horizons and optimization method still require further modification and validation based on specific geological conditions and field monitoring results in practical engineering applications, including refinement of the controlling load-bearing and energy-storage horizon and borehole parameters.

6. Conclusions

This study investigated the evolution mechanism of floor rockburst instability tendency in roadways with retained bottom coal and the optimization of borehole pressure-relief horizons through theoretical analysis and numerical simulation. A mechanical framework integrating structural stability analysis and the evolution of load-bearing and energy-storage states was established to reveal the influence mechanism of bottom coal thickness on floor instability tendency. The main conclusions are summarized as follows:

(1) Based on the equivalent transformed-section method, a stability analysis model for the bottom coal–floor composite structure was established. The results show that increasing bottom coal thickness increases the proportion of low-elastic-modulus bottom coal within the composite structure, resulting in a reduction in the equivalent flexural stiffness of the composite floor and a decrease in its resistance to horizontal extrusion deformation. Consequently, the instability tendency of the floor is enhanced.

(2) Variations in bottom coal thickness modify the stress transfer path and energy accumulation state within the roadway floor, causing the controlling load-bearing and energy-storage horizon to gradually migrate from the floor strata to the coal-rock composite zone and thick bottom coal zone. Based on the energy-stress index K, the load-bearing and energy-storage state of the composite floor was comprehensively characterized. The results indicate that, with increasing bottom coal thickness, the floor gradually evolves from a relatively stable load-bearing state toward a high energy-storage state. The increase in floor rockburst instability tendency results from the combined effects of reduced structural stability of the composite floor and adjustment of the load-bearing and energy-storage state.

(3) The key load-bearing and energy-storage zones of the floor differ under different bottom coal thickness conditions, and the effectiveness of borehole pressure relief depends on the matching between the borehole-affected zone and the controlling load-bearing and energy-storage zone of the floor. Floor borehole pressure relief should follow the strategy of "identifying the load-bearing and energy-storage horizon, weakening the key horizon, and adapting borehole depth accordingly", rather than simply increasing borehole depth or adopting a fixed empirical depth. The optimization results of pressure-relief horizons proposed in this study still require further validation considering specific geological conditions, field monitoring, and engineering practices.

Author Contributions: Conceptualization, W.L. and X.Z.; methodology, X.Z. and Z.O.; software, X.Z. and R.Z.; formal analysis, X.Z., R.Y. and S.M.; data curation, R.Z., R.Y. and G.L.; writing—original draft preparation, X.Z.; visualization, H.Y.; writing—review and editing, Y.W., P.X. and N.Z. All authors have read and agreed to the published version of the manuscript.

Funding: This research was funded by the National Natural Science Foundation of China (grant numbers 52274120 and 52374137) and the Key Program of Hebei Natural Science Foundation (grant number E2024508004).

Institutional Review Board Statement: Not applicable.

Informed Consent Statement: Not applicable.

Data Availability Statement: The data supporting the findings of this study are provided in the article and its Appendix A. The FISH function used to calculate the elastic strain energy density is provided in Appendix A, and the mechanical parameters of coal and rock before and after weakening are listed in Tables 1 and 3.

Conflicts of Interest: The authors declare no conflicts of interest.

Appendix A. FISH Function for Elastic Strain Energy Density Calculation

The elastic strain energy density of each zone was calculated based on the current principal stresses and elastic parameters according to Equation (8). The core FISH function used in the numerical calculation is provided below:

```
fish define tanxingneng
    z_p=zone.head
    loop while z_p#null
        E=zone.prop(z_p,'young')
        u=zone.prop(z_p,'poisson')
        s1=zone.stress.min(z_p)
        s2=zone.stress.int(z_p)
        s3=zone.stress.max(z_p)
        zone.extra(z_p,4)=(s1*s1+s2*s2+s3*s3-2*u*(s1*s2+s1*s3+s2*s3))/(2*E)
        z_p=zone.next(z_p)
    endloop
end
@tanxingneng
```

References

1. Tan, Y.L.; Tan, Y.; Guo, W.Y.; Li, B.; He, S.D.; Zhang, L.; Zhang, Y.J.; Zhang, Q.Y. Calculation model for kinetic energy and rock burst risk evaluation method during roadway excavation. *Int. J. Min. Sci. Technol.* **2025**, *35*, 677–690. [CrossRef]
2. Dou, L.M.; Mu, Z.L.; Li, Z.L.; Cao, A.Y.; Gong, S.Y. Research progress of monitoring, forecasting, and prevention of rockburst in underground coal mining in China. *Int. J. Coal Sci. Technol.* **2014**, *1*, 278–288. [CrossRef]
3. He, X.Q.; Zhou, C.; Song, D.Z.; Li, Z.L.; Cao, A.Y.; He, S.Q.; Khan, M. Mechanism and monitoring and early warning technology for rockburst in coal mines. *Int. J. Miner. Metall. Mater.* **2021**, *28*, 1097–1111. [CrossRef]
4. Liu, F.Y.; Dai, L.P.; Ju, M.H.; Hao, Y.Y.; Luo, S.; Wang, A.W.; Liu, G. An experimental study on the combined modification of coal with strong bursting liability using water injection and destressing boreholes under SHPB dynamic loading. *Measurement* **2026**, *276*, 121443. [CrossRef]
5. Wang, S.W.; Cao, A.Y.; Wang, C.B.; Guo, W.H.; Xue, C.C.; Liu, J.G.; Wu, X.S.; Shi, G.S. Mechanism of rockburst induced by the microseismic event in the floor strata of high tectonic stress zones: A case study. *Int. J. Coal Sci. Technol.* **2024**, *11*, 76. [CrossRef]
6. Xiao, Z.M.; Liu, J.; Gu, S.T.; Liu, M.Q.; Zhao, F.T.; Wang, Y.; Ou, C.; Zhen, M.Y. A control method of rock burst for dynamic roadway floor in deep mining mine. *Shock Vib.* **2019**, *2019*, 7938491. [CrossRef]
7. Cao, A.Y.; Zhu, L.L.; Du, Z.Y.; Liu, J.G.; Wang, Y. Control principle and pressure-relief technique of rock burst occurred in roadway floor. *J. Min. Saf. Eng.* **2013**, *30*, 848–855.
8. Liu, Y.B.; Zhu, S.T.; Zhang, X.F.; Wang, X.Y.; Li, Z.Q.; Zhou, J.Z.; Zhang, B.; Wang, G.A. Study on mechanism of pressure relief failure of bottom coal induced by strong vibration in driving face of thick coal seam. *J. Min. Strat. Control Eng.* **2024**, *6*, 053021. [CrossRef]
9. Ma, Q.; Tan, Y.L.; Liu, X.S.; Gu, Q.H.; Li, X.B. Effect of coal thicknesses on energy evolution characteristics of roof rock-coal-floor rock sandwich composite structure and its damage constitutive model. *Compos. Part B Eng.* **2020**, *198*, 108086. [CrossRef]
10. Zhang, R.P.; Gong, S.Y.; Shen, W.; Li, H.; Lu, Q. Mechanism of floor-type rockburst in steeply inclined ultra-thick coal seam under complex mining conditions: A case study. *Rock Mech. Rock Eng.* **2026**, *59*, 1319–1335. [CrossRef]
11. Xiao, Z.M.; Liu, J.; Wang, H.; Sun, L.; Zhou, H. Study on mechanism and control of rock burst instability of roadway floor induced by dynamic load disturbance. *Chin. J. Undergr. Space Eng.* **2019**, *15*, 1573–1581. [CrossRef]
12. Mu, Z.L.; Liu, G.J.; Yang, J.; Zhao, Q.; Javed, A.; Gong, S.K.; Cao, J.L. Theoretical and numerical investigations of floor dynamic rupture: A case study in Zhaolou Coal Mine, China. *Saf. Sci.* **2019**, *114*, 1–11. [CrossRef]
13. Zhang, D.; Bai, J.B.; Yan, S.; Wang, R.; Meng, N.K.; Wang, G.Y. Investigation on the failure mechanism of weak floors in deep and high-stress roadway and the corresponding control technology. *Minerals* **2021**, *11*, 1408. [CrossRef]
14. Zhou, J.L.; Pan, J.F.; Xia, Y.X.; Du, T.T.; Liu, W.A.; Zhang, C.Y. Mechanism and prevention of coal bursts in gob-side roadway floor under thick and hard roof in the deep mining area of Ordos. *Int. J. Coal Sci. Technol.* **2024**, *11*, 80. [CrossRef]
15. Liu, G.J.; Mu, Z.L.; Javed, A.; Gong, S.K.; Yang, J.; Cao, J.L. Investigation into mechanism of floor dynamic rupture by evolution characteristics of stress and mine tremors: A case study in Guojiahe Coal Mine, China. *Shock Vib.* **2018**, *2018*, 3279036. [CrossRef]
16. Feng, H.; Ma, X.; Zhao, Y.; Jiang, L.S.; Wen, X.L.; Cong, Q.; Wang, F.T. Research on the floor rockburst of panel entry under the mining influence: A case study. *Lithosphere* **2022**, *2022*, 6238642. [CrossRef]
17. Xu, X.F.; Dai, Z.; Xu, H. Study on the impact failure rules of roadway floor induced by dynamic load disturbance under extremely thick conglomerate. *ACS Omega* **2024**, *9*, 23542–23554. [CrossRef] [PubMed]

18. Wang, J.Y.; Shi, Q.W.; Guo, Z.J.; Wang, X.Y.; Wang, X.S.; Hong, A.K.; Sun, J.T. Investigation of floor rockburst mechanism based on simulation with FLAC3D. *J. North China Inst. Sci. Technol.* **2025**, *22*, 21–28. [CrossRef]
19. Tan, Y.L.; Song, S.L.; Zhang, X.F.; Liu, X.S. Safety evaluation method of bottom coal thickness in thick coal seam roadway. *Sci. Rep.* **2024**, *14*, 14812. [CrossRef] [PubMed]
20. Zhang, C.Y.; Pan, J.F.; Xia, Y.X.; Yang, G.Y.; Liu, S.H.; Lu, C. Influence mechanism and application analysis of bottom coal layer thickness on floor rock burst. *J. China Coal Soc.* **2020**, *45*, 3984–3994. [CrossRef]
21. Chen, F.; Dou, L.M.; Wang, G.F.; Xie, Q.; Xie, L. Effect of bottom coal thickness on roadway floor burst induced by dynamic disturbance in folded region. *Saf. Coal Mines* **2014**, *45*, 175–178, 182.
22. Chang, J.C.; Li, D.; He, K. Mining failure response characteristics of stope floor: A case of Renlou Coal Mine. *Adv. Civ. Eng.* **2020**, *2020*, 8832520. [CrossRef]
23. Mo, S.; Ramandi, H.L.; Oh, J.; Masoumi, H.; Canbulat, I.; Hebblewhite, B.; Saydam, S. A new coal mine floor rating system and its application to assess the potential of floor heave. *Int. J. Rock Mech. Min. Sci.* **2020**, *128*, 104241. [CrossRef]
24. Li, G.; Cao, A.Y.; Wang, G.F.; Bai, X.X.; Lyu, G.W.; Peng, Y.J.; Xie, Y.Q. Investigation of floor blasting for rock burst prevention in high-stress roadway under dynamic loading. *Sci. Rep.* **2025**, *15*, 38411. [CrossRef] [PubMed]
25. Su, R.Y.; Mu, Z.L.; Li, J.X.; Cao, J.L.; Jiang, C.L.; Ren, Y.Z.; Ji, J.Q.; Fu, H. Study on shaped charge blasting pressure-relief technology for the floor of extra-thick coal seams and its application. *Appl. Sci.* **2026**, *16*, 1079. [CrossRef]
26. Wang, H.J.; Liao, H.L.; Wei, J.; Liu, J.S.; Niu, W.L.; Liu, Y.W.; Guan, Z.C.; Sellami, H.; Latham, J.P. Stress release mechanism of deep bottom hole rock by ultra-high-pressure water jet slotting. *Pet. Sci.* **2023**, *20*, 1828–1842. [CrossRef]
27. Guo, D.M.; Kang, X.C.; Lu, Z.Y.; Chen, Q.Y. Mechanism and control of roadway floor rock burst induced by high horizontal stress. *Shock Vib.* **2021**, *2021*, 6745930. [CrossRef]
28. Chen, A.; Li, X.B.; Liu, X.S.; Tan, Y.L.; Xu, K.; Wang, H.L. "Relief-retaining" control technology of floor heave in mining roadway with soft rock: A case study. *Adv. Civ. Eng.* **2021**, *2021*, 1455052. [CrossRef]
29. Chen, T. Danger-relief principle and parameter optimization of borehole energy relief for rock burst in coal road floor. *Coal Sci. Technol.* **2023**, *51*, 21–31. [CrossRef]
30. Xu, X.F.; Dou, L.M.; Liu, J.; Cui, X.H.; Zhang, Y.L.; Yao, X.Y. Research of reasons and controlling for floor burst in coal mine roadway. *Rock Soil Mech.* **2010**, *31*, 1977–1982. [CrossRef]
31. Sun, X.M.; Miao, P.Y.; Shen, F.X.; Zhao, W.C.; Yang, M.H. Study on floor heave mechanism of horizontal layered soft rock roadway in deep well under different stress states. *J. Min. Saf. Eng.* **2018**, *35*, 1099–1106. [CrossRef]
32. Liu, H.W.; Ling, J.X.; Cao, M.L.; Wang, H.M. *Mechanics of Materials, Vol. I*; Higher Education Press: Beijing, China, 2017.
33. Shi, H.; Hao, B.Y.; Ren, X.Y.; Zhang, J. Mechanism and application of static stress intervention for controlled directional roof caving in fully mechanized mining faces. *Processes* **2025**, *13*, 1552. [CrossRef]
34. Peng, Y.J.; Wang, Q.; Cao, A.Y.; Xue, C.C.; Lyu, G.W.; Hao, Q.; Liu, Y.Q.; Bai, X.X.; Li, D. Mechanisms and influential factors of rock bursts in tunneling roadways of extra-thick coal seams. *Coal Geol. Explor.* **2024**, *52*, 25–39. [CrossRef]
35. Zhong, T.P.; Li, Z.L.; He, X.Q.; Song, D.Z.; Hu, X.C.; Liu, X.D.; Zhou, C. Research on rock burst prevention by shallow rock mass weakening in steeply inclined and extremely thick coal seams. *J. Min. Strat. Control Eng.* **2024**, *6*, 20–33. [CrossRef]

Disclaimer/Publisher's Note: The statements, opinions and data contained in all publications are solely those of the individual author(s) and contributor(s) and not of MDPI and/or the editor(s). MDPI and/or the editor(s) disclaim responsibility for any injury to people or property resulting from any ideas, methods, instructions or products referred to in the content.